HHS Public Access

Author manuscript

Proc SPIE Int Soc Opt Eng. Author manuscript; available in PMC 2016 April 26.

Published in final edited form as:

Proc SPIE Int Soc Opt Eng. 2016 February 27; 9784: . doi:10.1117/12.2216994.

On the Fallacy of Quantitative Segmentation for T1-Weighted MRI

Andrew J. Plassard[a], **Robert L. Harrigan**[b], **Allen T. Newton**[c], **Swati Rane**[d], **Srivatsan Pallavaram**[b], **Pierre F. D'Haese**[b], **Benoit M. Dawant**[a,b], **Daniel O. Claassen**[e], and **Bennett A. Landman**[a,b,c]

Andrew J. Plassard: Andrew.J.Plassard@vanderbilt.edu

[a]Computer Science, Vanderbilt University, 2301 Vanderbilt Place, Nashville, TN USA 37235

[b]Electrical Engineering, Vanderbilt University, 2301 Vanderbilt Place, Nashville, TN USA 37235

[c]Radiology, Vanderbilt University, 2301 Vanderbilt Place, Nashville, TN USA 37235

[d]Neurology, University of Washington, Seattle WA USA 98195

[e]Neurology, Vanderbilt University, 2301 Vanderbilt Place, Nashville, TN USA 37235

Abstract

T1-weighted magnetic resonance imaging (MRI) generates contrasts with primary sensitivity to local T1 properties (with lesser T2 and PD contributions). The observed signal intensity is determined by these local properties and the sequence parameters of the acquisition. In common practice, a range of acceptable parameters is used to ensure “similar” contrast across scanners used for any particular study (e.g., the ADNI standard MPRAGE). However, different studies may use different ranges of parameters and report the derived data as simply “T1-weighted”. Physics and imaging authors pay strong heed to the specifics of the imaging sequences, but image processing authors have historically been more lax. Herein, we consider three T1-weighted sequences acquired the same underlying protocol (MPRAGE) and vendor (Philips), but “normal study-to-study variation” in parameters. We show that the gray matter/white matter/cerebrospinal fluid contrast is subtly but systemically different between these images and yields systemically different measurements of brain volume. The problem derives from the visually apparent boundary shifts, which would also be seen by a human rater. We present and evaluate two solutions to produce consistent segmentation results across imaging protocols. First, we propose to acquire multiple sequences on a subset of the data and use the multi-modal imaging as atlases to segment target images any of the available sequences. Second (if additional imaging is not available), we propose to synthesize atlases of the target imaging sequence and use the synthesized atlases in place of atlas imaging data. Both approaches significantly improve consistency of target labeling.

Keywords

Multi-Atlas Segmentation; Image Synthesis; T1-Weighting

Correspondence to: Andrew J. Plassard, Andrew.J.Plassard@vanderbilt.edu.

1. Introduction

T1-weighted MRI derives contrast from the local T1, T2, and Proton Density (PD) of the imaging subject. The signal intensity is then read out as a function of those tissue characteristics and the sequence definition. In some cases, such as the Alzheimer's Disease Neuroimaging Initiative (ADNI), very strict sequence definitions are available to insure data consistency [1]. On the other hand, many studies consider cross-site, scanner, or sequence analyses but do not necessarily consider the effect those changes may have on the imaging [2]. Further, perceived anatomic differences may be visually present both to humans and automated techniques, derived from the subtle changes in the imaging sequence parameters (Figure 1). Thus these changes may result in systematic differences in study results depending on the sequence used and the techniques used for analyzing and processing the data.

To quantitatively investigate this problem, we begin with a simple assumption that a particular algorithm has been accepted as sufficiently accurate for a single T1-weighted MRI acquisition. Specifically, we assume that the multi-method of Asman et al [3, 4] with the widely used BrianCOLOR atlases is representative of an ADNI compliant 3T MPRAGE (herein "TI - 891"). Note that this specific assumption has been made by others, e.g., [5]. We then look at two other, similar 3T MPRAGE sequences with slightly different acquisition parameters, but that were also designed and used for research into whole-segmentation (herein, "TI - 624" and "TI - 927" with details to follow).

The remainder of this paper is organized as follows. First we describe the data acquisition sequences used for both application and validation. Second, we propose a solution using our acquired dataset as atlas with comparable sequences for segmentation. Third, we present a quantitative solution to the problem of varying sequence acquisitions where we start from the foundational signal equations defining MPRAGE signal and we synthesize new atlas images better matching the contrast of our target images. We validate both of these methods against a reference segmentation and show that both presented techniques show significant improvement when using atlases of the same sequence when compared to atlases of differing sequences.

2. Methods and theory

This section is organized as follows. First we describe our acquired dataset where each subject was scanned with three T1-weighted MPRAGE sequences. Second, we describe our protocol for image synthesis using a standard Dual Spin Echo image and MPRAGE with known sequence parameters. Third, we characterize the open-access dataset used for synthetic atlas generation and the synthesized atlases. Last, we describe the procedure used for segmentation in the results.

Data Acquisition

Data for seven subjects (6 male, 1 female, ages 21–62) were acquired particularly for this study. Each subject was scanned with three unique sequences on a single trip into the scanner. All scans were acquired on a 3T Philips Achieva MRI (Philips Medical Systems,

Best, The Netherlands) with a 32-channel receive coil. The first acquisition sequence was an MPRAGE T1-weighted MRI with TR/TE/TI/flip angle 7.9/3.65/927ms/5°. The second acquisition sequence was an MPRAGE T1-weighted MRI with TR/TE/TI/flip angle – 8.2/3.7/891ms/8°. The third acquisition sequence was an MPRAGE T1-weighted MRI with TR/TE/TI/flip angle – 8.9/4.6/624ms/8°. For the remained of this work we refer to these different sequences by their inversion time (TI – 927, TI – 891, and TI – 624 respectively), and we note that the second acquisition fits within the ADNI standards for an MPRAGE sequence [1]. After acquisition, for each subject TI – 927 and TI – 624 were rigidly registered to TI – 891 with NiftyReg to create a consistent space [6].

Image Synthesis

The goal of image synthesis is to generate new atlases with pulse sequence parameters more closely related to the target image than the target image. To do this, we start with the MPRAGE equation defined by Deichmann et al [7]

$$S_M(x)=G_M PD(x)\left(1-\frac{2e^{-\frac{TI}{T_1(x)}}}{1+e^{-\frac{TI+TD+\tau}{T_1(x)}}}\right) \quad (1)$$

where $S_M(x)$ is the signal from the MPRAGE sequence at location x, G_M is the scanner gain, $PD(x)$ is the proton density at x, TI is the inversion time, TD is the delay time, τ is the slice timing, and $T_1(x)$ is the T1-relaxation time at x. In order to synthesize a new image with new pulse parameters thus we must know $PD(x)$ and $T_1(x)$. To estimate $PD(x)$ we begin with a Dual Spin Echo sequence which has signal is defined as [8]

$$S_{DSE_n}(x)=G_{DSE}PD(x)\left(1-2e^{-\frac{TR-\frac{TE_1+TE_2}{2}}{T_1(x)}}+2e^{-\frac{TR-\frac{TE_2}{2}}{T_1(x)}}-e^{-\frac{TR}{T_1(x)}}\right)e^{-\frac{TE_n}{T_2(x)}} \quad (2)$$

where $S_{DSE_n}(x)$ is the signal from the nth echo time at voxel x, G_{DSE} is the scanner gain for the Dual Echo sequence, and TE_n is the echo time for the nth echo. If we assume TR is significantly greater than TE, which is standard practice for Dual Echo sequences, the component of the signal effected by $T_1(x)$ approaches 1 and the equation reduces to

$$S_{DSE_n}(x)=G_{DSE}PD(x)e^{-\frac{TE_n}{T_2(x)}} \quad (3)$$

from which we can solve for $T_2(x)$ as

$$T_2(x)=\frac{TE_1-TE_2}{\ln\left(S_{DSE_2}(x)\right)-\ln\left(S_{DSE_1}(x)\right)} \quad (4)$$

which is the slope of the log-fit of the echo times. From this solution we solve for $G_{DSE}PD(x)$ by

$$G_{DSE}PD(x)=\frac{S_{DSE_1}}{e^{-\frac{TE_1}{T_2(x)}}} \quad (5)$$

which is simply a constant factor times $PD(x)$. With a solution for $PD(x)$ we can now solve for the remaining parameters in (1). First we solve for G_M as

$$\frac{S_M(x)}{G_{DSE}PD(x)}=\frac{G_M PD(x)}{G_{DSE}PD(x)}\left(1-\frac{2e^{-\frac{TI}{T_1(x)}}}{1+e^{-\frac{TI+TD+\tau}{T_1(x)}}}\right) \quad (6)$$

$$\frac{S_M(x)}{G_{DSE}PD(x)}=G_N\left(1-\frac{2e^{-\frac{TI}{T_1(x)}}}{1+e^{-\frac{TI+TD+\tau}{T_1(x)}}}\right) \quad (7)$$

where G_N is simply $\frac{G_M}{G_{DSE}}$ since neither parameter needs to be explicitly solved for. Thus G_N can be solved as

$$G_N=\frac{S_M(x)\left(1+e^{-\frac{TI+TD+\tau}{T_1(x)}}\right)}{G_{DSE}PD(x)\left(1-2e^{-\frac{TI}{T_1(x)}}\right)} \quad (8)$$

Though this equation still contains the parameter $T_1(x)$ we simply use the median intensity of the gray matter, white matter, and csf with known T1-relaxation values for these regions to estimate the gain and take the average gain from those estimates [9]. To estimate the T1-relaxation, since in typical T1-weighted imaging is on the order of hundreds of milliseconds and TD and τ are typically on the order of milliseconds for 3T T1-weighted sequences, we assume that $e^{-\frac{TI+TD+\tau}{T_1(x)}} \approx e^{-\frac{TI}{T_1(x)}}$ and thus $T_1(x)$ we solve for in closed form as follows from (1)

$$\frac{2e^{-\frac{TI}{T_1(x)}}}{1+e^{-\frac{TI}{T_1(x)}}}=1-\frac{S_M(x)}{G_M PD(x)G_N} \quad (9)$$

For simplicity we define

$$S=1-\frac{S_M(x)}{G_M PD(x)G_N} \quad (10)$$

for the remainder of the derivation. Continuing from (9) with the simplification

$$2e^{-\frac{TI}{T_1(x)}}=S+Se^{-\frac{TI}{T_1(x)}} \quad (11)$$

$$e^{-\frac{TI}{T_1(x)}}=\frac{S}{2-S} \quad (12)$$

$$-\frac{TI}{T_1(x)}=\ln\left(\frac{S}{2-S}\right) \quad (13)$$

$$T_1(x)=-\frac{\mathrm{TI}}{\ln\left(\frac{S}{2-S}\right)} \quad (14)$$

By solving for the parameters, $G_{DSE}PD(x)$ and $T_1(x)$, we can use (1) to synthesize new T1-weighted MPRAGE images.

Synthetic Atlas Generation

To generate synthetic atlas images we consider the Multi-Modal Kirby21 open-source data resource since it has the requisite Dual Echo (TR/TE1/TE2=6653ms/30ms/80ms) and MPRAGE (TR/TE/TI=6.7/3.1/842ms) for synthesis [10]. All images were bias corrected with the N4 bias correction algorithm as a preprocessing step [11]. 10 subjects with T2-relaxation times most closely matching the known times for gray matter and what matter were selected for synthesis [9]. Synthetic images were generated on the selected images to match the three acquired atlas sets (TI – 624, TI – 891, and TI – 927). Example results for the intermediary calculations of PD, T1-relaxation, and T2-relaxation can be seen in Figure 2.

Multi-Atlas Segmentation

All multi-atlas segmentations in this study follow an identical procedure. Atlas and target images are first bias corrected with the N4 Bias Correction algorithm [11]. Altas images are then non-rigidly registered to the target image with the Advanced Normalization Tools package and the Symmetric Image Normalization Algorithm (SyN) [12]. Image and label volumes for the atlas were then deformed to the target space with bi-cubic and nearest-neighbor interpolation respectively. After deformation, the registered label volumes were fused together with Non-Local Spatial STAPLE [3, 4].

For initial segmentations of both the acquired data and the synthesis data, 45 OASIS atlases were used from the 2013 MICCAI multi-atlas segmentation challenge [13]. These atlases are defined as anatomically consistently with images following the ADNI protocol (TI – 891 in our case) [1, 5]. For all of the acquired data and the Kirby 21 synthesis images, we performed a multi-atlas segmentation using the above procedure but only selecting the 15 geodesically closest atlases for fusion.

3. Results

Multi-Acquisition Multi-Atlas Segmentation

For the seven subjects with three T1-weighted images acquired, we co-registered each subject's scans to their TI – 891 [6]. We then segmented TI – 891 for each subject with the previously defined procedure for multi-atlas segmentation. In a leave-one-out study, we then segmented each acquisition for each subject with its paired acquisitions and separately with

the TI – 891's resulting in five sets of segmentations per subject (i.e., TI – 624 segmented with TI 624, TI – 624 segmented with TI – 891, TI – 891 segmented with TI – 891, TI – 927 segmented with TI – 927, and TI – 927 segmented with TI – 891). We then calculated the volumes of cortical gray matter, subcortical gray matter, and cerebral white matter for each of the five segmentations. Using TI – 891 segmented with TI – 891 as the reference value of the "true" volume, TI – 624 segmented with TI – 624 and TI – 927 segmented with TI – 927 outperformed TI – segmented with TI – 891 and TI – 927 segmented with TI – 891 respectively (figure 3; * indicates values were significantly closer to 1 than their counterpart, Wilcoxon sign-rank test). This result shows that though the anatomic boundaries differ in perception between the sets of scans, we can still produce segmentations more consistent with the desired boundaries by using a sequence more closely matching our target.

Image Synthesis Multi-Atlas Segmentation

We selected ten subjects from the Kirby 21 open-access data resource and used their Dual Spin Echo and MPRAGE acquisitions for synthesis [10]. For each of the ten Kirby 21 subjects, we synthesized MPRAGE images with sequence parameters comparable to our acquired data (i.e. TI – 624, TI – 891, TI – 927). We then performed a multi-atlas segmentation between each set of newly synthesized atlases and our previously acquired data (see above), resulting in 9 segmentations for each of our seven subjects. For cortical segmentation of all acquisitions, using the synthetic atlas with an identical sequence to the target acquisition produced significant improvements over or comparable results to the segmentations with other synthetic atlases. For white matter segmentation, TI – 927 and TI – 624 showed significant improvements when using their matched synthetic atlases but interestingly TI – 891's white matter volume was closest to the target volume when segmented by atlases with TI – 927. In subcortical volume TI – 927 and TI – 891 did not show any significant improvement based on synthetic atlas selection whereas TI – 624 segmented by TI – 624 produced segmentation volumes significantly closer to the target volume than with the other synthetic sequences (figure 4).

4. Discussion

In this work we evaluate the importance of T1-weighted MRI sequence variant in image processing work. We show significant perceived differences in structural information between scans of the same subject under different MRI sequence parameters. We then show that, if using structural information consistent with a target sequence variant and atlases of a sequence more similar to a target sequence, segmentation results are more parsimonious with the expectation than if we use atlases of an alternate variant. We also consider synthesizing atlas images of the ideal sequence variant from the underlying biological signals of T1-weighted MRI. We show that by generating synthetic atlases more similar to the target image we typically produce segmentation volumes more parsimonious with the target volume.

Acknowledgments

This project was supported by the National Center for Research Resources, Grant UL1 RR024975-01 (now at the National Center for Advancing Translational Sciences, Grant 2 UL1 TR000445-06), the Michael J. Fox Foundation,

and NSF CAREER 1452485. The content is solely the responsibility of the authors and does not necessarily represent the official views of the NIH. This work was conducted in part using the resources of the Advanced Computing Center for Research and Education at Vanderbilt University, Nashville, TN.

REFERENCES

1. Jack CR, et al. The Alzheimer's disease neuroimaging initiative (ADNI): MRI methods. Journal of Magnetic Resonance Imaging. 2008; 27(4):685–691. [PubMed: 18302232]
2. Tustison NJ, et al. Large-scale evaluation of ANTs and FreeSurfer cortical thickness measurements. Neuroimage. 2014; 99:166–179. [PubMed: 24879923]
3. Asman AJ, Landman BA. Formulating spatially varying performance in the statistical fusion framework. IEEE Trans Med Imaging. 2012; 31(6):1326–1336. [PubMed: 22438513]
4. Asman AJ, Landman BA. Non-local statistical label fusion for multi-atlas segmentation. Med Image Anal. 2013; 17(2):194–208. [PubMed: 23265798]
5. Davatzikos C, Guray Erus XD, Doshi J. Hierarchical Parcellation of MRI using multi-atlas labeling methods.
6. Ourselin S, et al. Reconstructing a 3D structure from serial histological sections. Image and vision computing. 2001; 19(1):25–31.
7. Deichmann R, et al. Optimization of 3-D MP-RAGE sequences for structural brain imaging. Neuroimage. 2000; 12(1):112–127. [PubMed: 10875908]
8. Bernstein, MA.; King, KF.; Zhou, XJ. Handbook of MRI pulse sequences. Elsevier; 2004.
9. Wansapura JP, et al. NMR relaxation times in the human brain at 3.0 tesla. Journal of magnetic resonance imaging. 1999; 9(4):531–538. [PubMed: 10232510]
10. Landman BA, et al. Multi-parametric neuroimaging reproducibility: a 3-T resource study. Neuroimage. 2011; 54(4):2854–2866. [PubMed: 21094686]
11. Tustison NJ, et al. N4ITK: improved N3 bias correction. Medical Imaging, IEEE Transactions on. 2010; 29(6):1310–1320.
12. Avants BB, et al. Symmetric diffeomorphic image registration with cross-correlation: evaluating automated labeling of elderly and neurodegenerative brain. Med Image Anal. 2008; 12(1):26–41. [PubMed: 17659998]
13. Asman A, et al. Miccai 2013 segmentation algorithms, theory and applications (SATA) challenge results summary. MICCAI Challenge Workshop on Segmentation: Algorithms, Theory and Applications (SATA). 2013

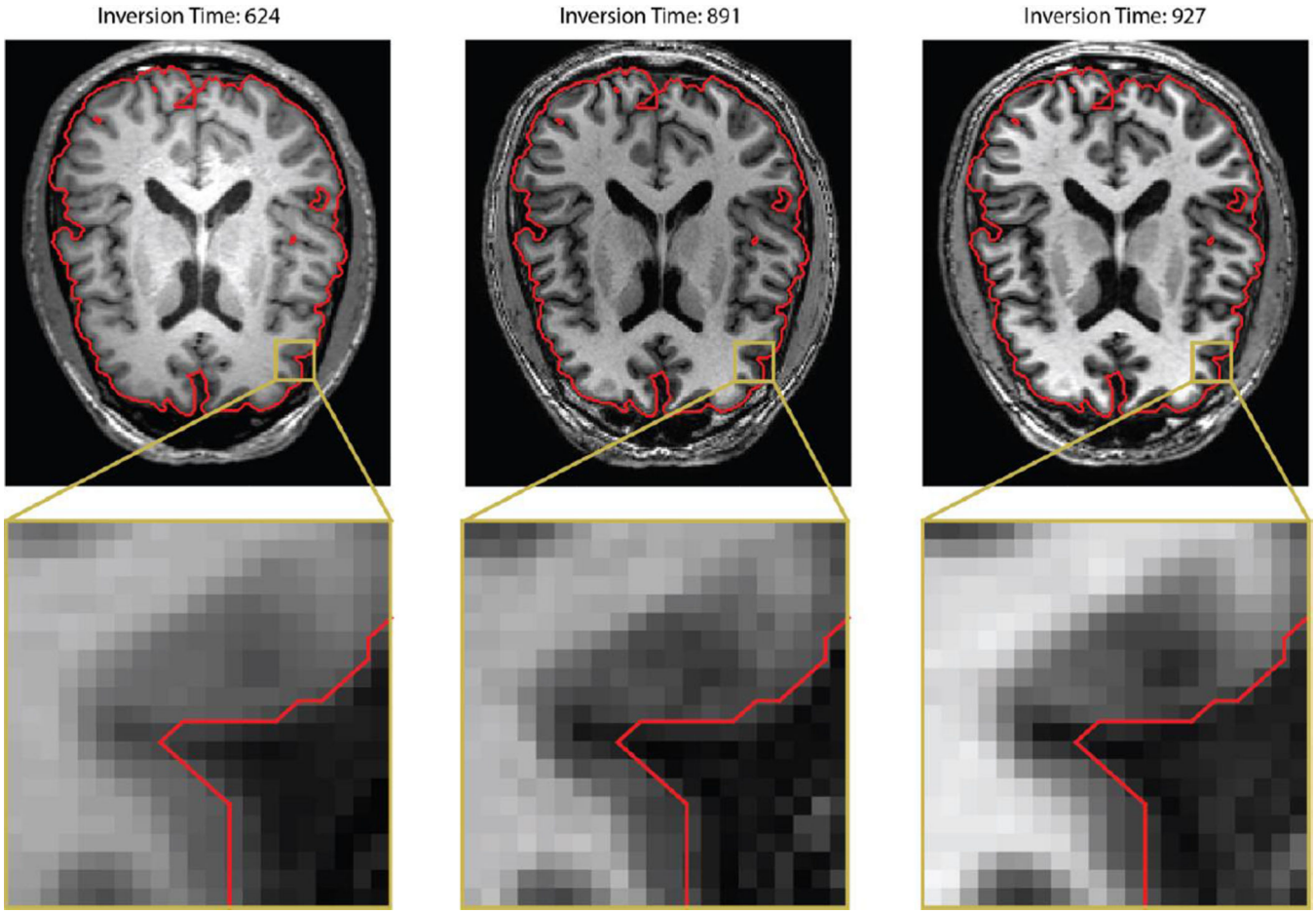

Figure 1.

Example segmentation results for three T1-weighted MPRAGE sequences with different inversion times. The red line corresponds to the contour of the segmentation on TI - 891. The perceived boundary on the zoomed-in images appears to dramatically shift and a human labeler or automated algorithm with no knowledge of the imaging protocol would clearly define different gray matter/csf boundaries for each imaging sequence.

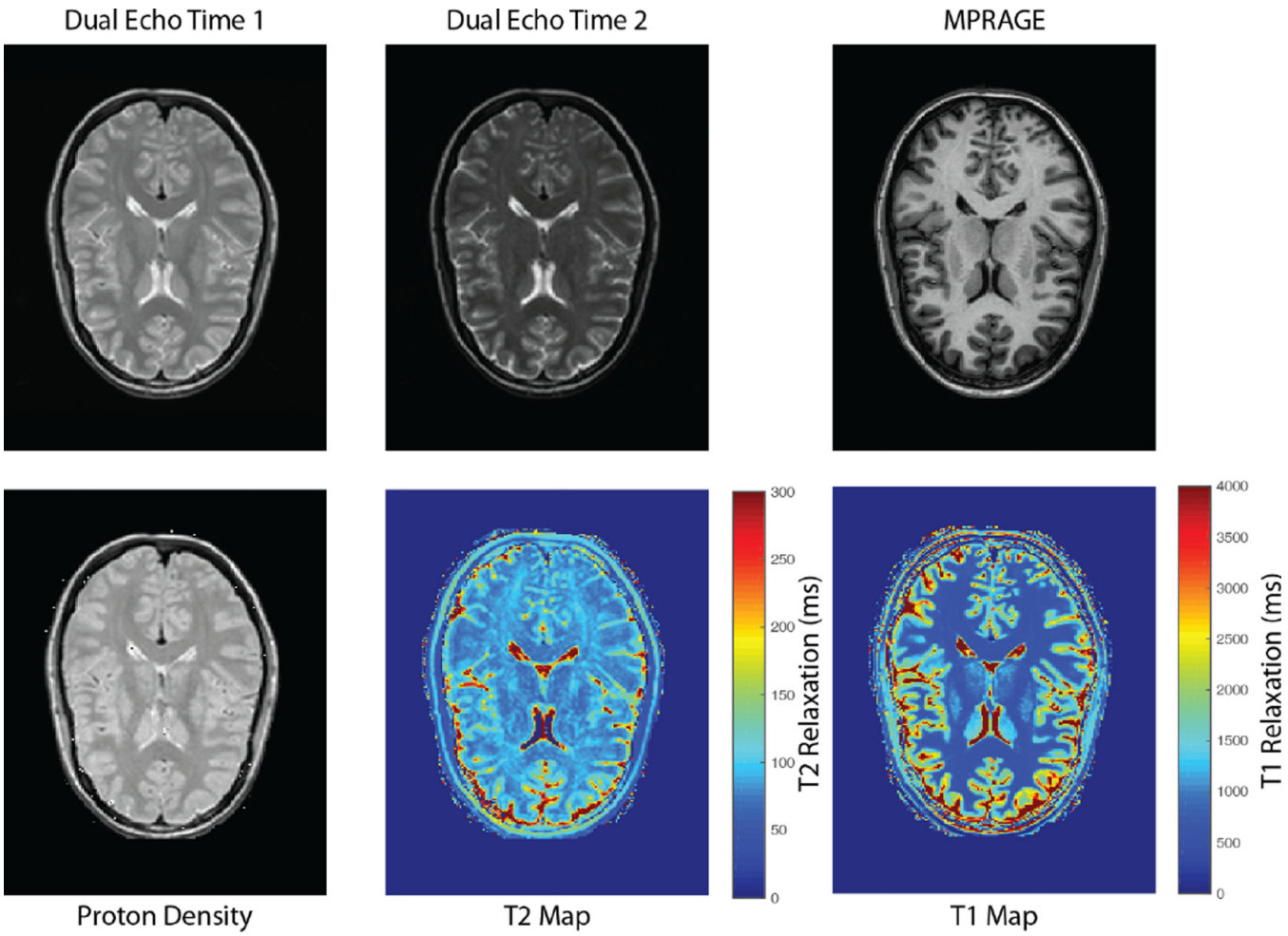

Figure 2.

Intermediary results from image synthesis. The cited values for T2-relaxation in gray matter, white matter are approximately 100 and 80 ms respectively. The cited values for T1-relaxation in the gray matter and white matter are approximately 1350 and 800 ms respectively. These values appear consistent with the intermediary results of image synthesis.

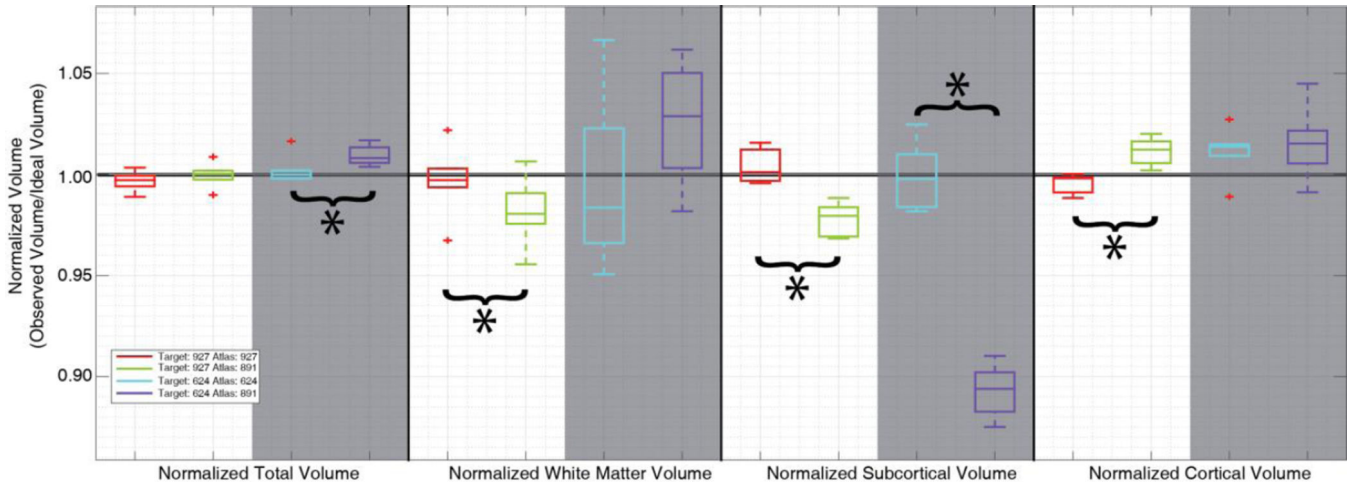

Figure 3.

Quantitative segmentation results from the multi-sequence acquisition segmentations. Segmentation volumes were normalized to the volume of TI – 891 segmented with TI – 891 to provide a normalized target volume for visualization. Normalizing to TI – 891 as a reference volume defines a value of 1 as the "correct" volume for each region of interest. * between two boxplots indicates a significant difference ($p<0.05$ Wilcoxon sign-rank test)

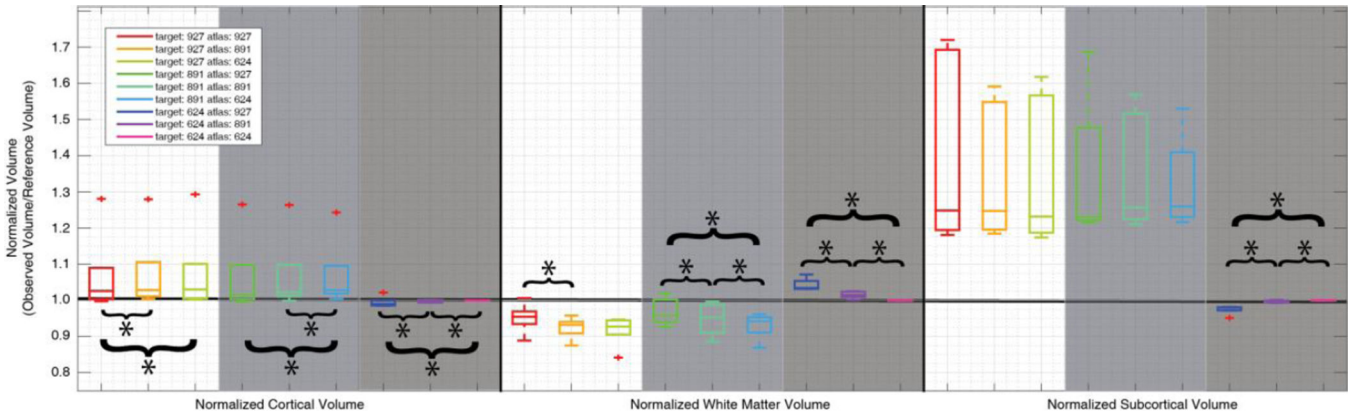

Figure 4.

Volumetric segmentation volumes for multi-atlas segmentation with image synthesis. Region volumes are normalized to volume of TI – 891's initial segmentation. We note that this is a reference point for comparison and results closer to 1 do not necessarily indicate more accurate segmentations. Across the three sets of structures, segmentation volumes differ significantly depending on the synthesized sequence parameters of the atlases and in most cases using the atlas sequence most closely matching the target produces significant improvements over the segmentation results (* between boxplots indicates $p<0.05$, Wilcoxon sign-rank test).